Humic Acid-Induced Silver Nanoparticle Formation Under Environmentally Relevant Conditions

Nelson Akaighe,[†] Robert I. MacCuspie,[‡] Divina A. Navarro,[§] Diana S. Aga,[§] Sarbajit Banerjee,[§] Mary Sohn,[†] and Virender K. Sharma[†,*]
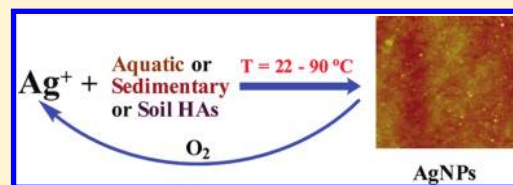
[†]Chemistry Department, Florida Institute of Technology, 150 West University Boulevard, Melbourne, Florida 32901, United States

[‡]Material Measurement Laboratory, National Institute of Standards and Technology, 100 Bureau Drive, Stop 8520, Gaithersburg, Maryland 20899-8520, United States

[§]Department of Chemistry, 410 Natural Sciences Complex, University at Buffalo, The State University of New York, Buffalo, New York 14260-3000, United States

Ⓢ *Supporting Information*

ABSTRACT: The formation of silver nanoparticles (AgNPs) via reduction of silver ions (Ag$^+$) in the presence of humic acids (HAs) under various environmentally relevant conditions is described. HAs tested originated from the Suwannee River (SUW), and included samples of three sedimentary HAs (SHAs), and five soils obtained across the state of Florida. The time required to form AgNPs varied depending upon the type and concentration of HA, as well as temperature. SUW and all three SHAs reduced Ag$^+$ at 22 °C. However, none of the soil HAs formed absorbance-detectable AgNPs at room temperature when allowed to react for a period of 25 days, at which time experiments were halted. The appearance of the characteristic surface plasmon resonance (SPR) of AgNPs was observed by ultraviolet−visible spectroscopy in as few as 2−4 days at 22 °C for SHAs and SUW. An elevated temperature of 90 °C resulted in the accelerated appearance of the SPR within 90 min for SUW and all SHAs. The formation of AgNPs at 90 °C was usually complete within 3 h. Transmission electron microscopy and atomic force microscopy images showed that the AgNPs formed were typically spherical and had a broad size distribution. Dynamic light scattering also revealed polydisperse particle size distributions. HAs appeared to colloidally stabilize AgNPs based on lack of any significant change in the spectral characteristics over a period of two months. The results suggest the potential for direct formation of AgNPs under environmental conditions from Ag$^+$ sources, implying that not all AgNPs observed in natural waters today may be of anthropogenic origin.

INTRODUCTION

In recent years, there has been growing interest in the manufacture of silver nanoparticles (AgNPs) due to their antibacterial and antiviral properties, in addition to numerous industrial applications including heterogeneous catalysis, cosmetics, microelectronics, and conductive inks and adhesives.[1−3] This increase in production of AgNPs has caused both regulatory and public health[4] concerns, because there is unknown risk to microbial communities and to ecosystems. Risk could arise through either a novel mechanism unique to the AgNPs itself, such as those reported with zebrafish embryos,[5,6] or the large surface area to volume ratio of the AgNPs could exhibit increased rates of release of silver ions (Ag$^+$), a legacy pollutant from the mining[7] and photographic industries.[8,9] The toxicity of AgNPs is strongly affected by colloidal stability, size, exposed crystallographic facets, surface chemistry and morphology.[10,11] Therefore, several studies have recently been conducted to increase the understanding of the impact of environmental conditions such as pH, ionic strength, and electrolyte composition on the surface charge and aggregation behavior of silver nanoparticle suspensions.[12,13]

Significant progress has been accomplished with respect to understanding the behavior of AgNPs under natural environmental conditions, but no study on the direct formation of AgNPs in aquatic systems has been reported. However, the presence of colloidal silver in coastal areas was reported in the mid 1990s before widespread adoption of AgNPs in consumer products.[14] While this previous study described the presence of colloidal silver, it did not establish the sizes or morphologies of the colloidal particles or provide a mechanism of how they were formed. Therefore, this paper aims to examine the potential formation of AgNPs in the environment, and reports for the first time the formation of AgNPs by the reduction of Ag$^+$ by humic acids (HAs) at room temperature (RT).

Ag$^+$ usually enters the aquatic environment from industrial and municipal water treatment plants.[15,16] Total silver in environmental water samples has been reported to be in the range of one to hundreds of ng L^{-1}.[17] Reduction of Ag$^+$ by peat fulvic acid at a high concentration of 500 mg L^{-1} and elevated temperatures (70−90 °C) to form AgNPs, confirmed only by UV-vis spectroscopy, has been reported.[18] However, the reduction of Ag$^+$ by peat

fulvic acid was only considered as a new synthetic approach in synthesizing AgNPs as bactericides for medical applications. Furthermore, no evidence for induced crystallinity of the purported colloids was reported. This research focuses on HAs as an important fraction of organic matter with high molecular weight distribution, which is base soluble but insoluble at low pH (pH < 2.0). HAs contain functionalities, such as phenolic—OH, quinones, hydroxyls, methoxyls, aldehydes, ketones, enolic—OH,[19] and thiols[20] which could serve as reduction sites for metal ions. In the current paper, HA appears to act as both a reducing and capping agent at environmentally relevant conditions, and further endows colloidal stability to the synthesized AgNPs by preventing agglomeration. The distinctive role evidenced for HA's from different sources also suggests clear structure—function correlations hitherto not considered in the literature.

The major focus of this paper is to demonstrate the formation of AgNPs by the reduction of Ag^+ with HA. The use of HA from different sources may promote an understanding of the role of aromatic versus aliphatic contents of HA in the formation of AgNPs.[21,22] Soil HAs have more aromatic structures, contain far less aliphatic structures, and have a more oxidized form of organic sulfur.[23] Soil HAs are derived from slow microbial decomposition of lignin containing terrestrial plants.[24] On the other hand, sedimentary and aquatic HAs have more aliphatic structures and are far less aromatic, owing to their formation from the decomposition of algal or bacterial residues. SHAs also contain the reduced form of organic sulphides (thiols) which may be involved in reduction of metal ions.[20] The formation of AgNPs was studied using ultraviolet-visible spectroscopy (UV-vis) to monitor the appearance of the characteristic surface plasmon resonance (SPR) absorption. Analyses were conducted over a wide temperature range (22—90 °C) to include temperatures which would be relevant to hot-springs and waters in thermal areas that are naturally at elevated temperatures. Additionally, the U.S. Environmental Protection Agency reports the concentration of silver in water from certain hot-springs to be 43 mg L^{-1} (0.40 mmol L^{-1}),[25] which is considerably greater than the lowest concentrations of silver used in the current paper that were found to produce AgNPs when exposed to HAs. The size, crystallinity, and morphology of the formed AgNPs were determined by collecting dynamic light scattering (DLS) data, atomic force microscopy (AFM) and transmission electron microscopy (TEM) images.

■ MATERIALS AND METHODS

Chemicals. Silver nitrate with >99.0% purity was purchased from Sigma Aldrich (St. Louis, MO) and used as received without further purification. Suwannee River HA (SUW), from an aquatic source, was purchased from the International Humic Substances Society (IHSS, St. Paul, MN). Other SHAs used were isolated and purified from fresh water and marine sediments. Standard procedures were used in isolation and purification of the HAs in accordance with IHSS guidelines.[26,27] All HAs except those purchased were isolated from soils and sediments in the state of Florida. SHAs used in this study included Sebastian River (SR) and Lake Delancy (LD) samples, both from fresh water sediments and M2 from marine sediments. The soil HAs were from Melbourne Beach (MB), Florida Institute of Technology Jungle (FITJ), a woody area in Melbourne (S1), and West Melbourne (WM). A soil HA was purchased from Aldrich (AL), (product number H16752). In this study, sodium phosphate (5 mmol L^{-1})/sodium borate (1 mmol L^{-1}) buffer solution with initial pH of 9.0 was used to make standard solutions of all HAs except (SUW-1). EPA MHRW (moderately hard reconstituted water, synthetic freshwater)[28] with

pH 7.8 containing calcium, magnesium, sodium, potassium, chloride, bicarbonate, and sulfate ions was used to prepare SUW-1 solution. The pH of all HA solutions ranged from 7.4 to 8.1 (Table S1 in the Supporting Information (SI)). All pH measurements were performed on an Orion pH/ISEmeter, model 710A (Thermo Fisher Scientific, Waltham, MA).

Synthesis Method. AgNPs were formed by the reduction of silver nitrate with HA (this can also be conceptualized as oxidation of the HA). The HA concentrations varied from (1—100) mg L^{-1}. The silver nitrate concentration was varied from 10 μmol L^{-1} to 1 mmol L^{-1}. The reaction temperature varied from RT (22 ± 1 °C) up to 90 ± 1 °C. Typically, 2 mL of HA solution was added to 2 mL of silver nitrate solution, and the reaction mixture was either stirred at RT under normal laboratory lighting in capped clear glass tubes for periods up to several days or was heated for several hours depending on the concentration and source of the HA. The reaction progress was monitored at regular intervals by UV-vis spectroscopy. The extent of reduction of Ag^+ to AgNPs varied from 0.6 to 5%, which has been estimated based on the measured absorbance of standard AgNP solutions (SI Figure SI-13) and the number of Ag atoms within a 14 nm nanocrystals deduced from known crystallographic parameters. Visual and spectroscopic examination of the HA/Ag mixtures confirmed that the HA completely dissolved in the buffer solution and UV-vis spectra of the HA used in experiments remained similar during the experimental duration. No indication of scattering peaks was seen in the UV-vis spectra as have been observed in other experiments in our laboratory when HA was precipitated at acidic or high ionic strength conditions.

UV-Vis Spectroscopy. UV-vis measurements were acquired using 1 cm optical path length quartz cuvettes on an Agilent Technologies 8453 GA11034 spectrometer (Santa Clara, CA). All measurements were performed at RT. Aliquots removed from samples at elevated temperatures were cooled by holding the cuvette under running tap water for 3 min to equilibrate to RT before measurement. Blanks consisted of sodium phosphate/sodium borate buffer solution without HAs, as true environmental samples have varying HA compositions and therefore could not be accurately subtracted. Reactions were analyzed until absorbance was measured to be approximately 2.0.

Dynamic Light Scattering (DLS). DLS measurements were performed in accordance with established standard protocol NIST and National Cancer Institute Nanotechnology Characterization Laboratory (NIST-NCL) Assay Cascade PCC-1.[29] Details of procedure are given (SI Text SI-1).

Transmission Electron Microscopy (TEM). High resolution TEM (HRTEM) and selected area electron diffraction (SAED) were performed using a JEOL (Tokyo, Japan) JEM-2010 instrument with an accelerating voltage of 200 kV. Samples were prepared by slow evaporation of solution onto a 400-mesh Carbon/Formvar TEM grid (Electron Microscopy Sciences, Hatfield, PA).

Atomic Force Microscopy. NIST-NCL Assay Cascade protocol PCC-6 was followed to avoid sample drying induced agglomeration.[30] Details of procedure are given (SI Text SI-2).

■ RESULTS AND DISCUSSION

Formation of AgNPs. The initial experiments on the formation of AgNPs by HA were carried out using SUW. The color of the reaction mixture under various reaction conditions changed with time from a pale yellow characteristic of the HA solution to an intense yellow characteristic of the SPR of AgNPs. The SPR peak wavelength was approximately 400 nm recorded by UV-vis
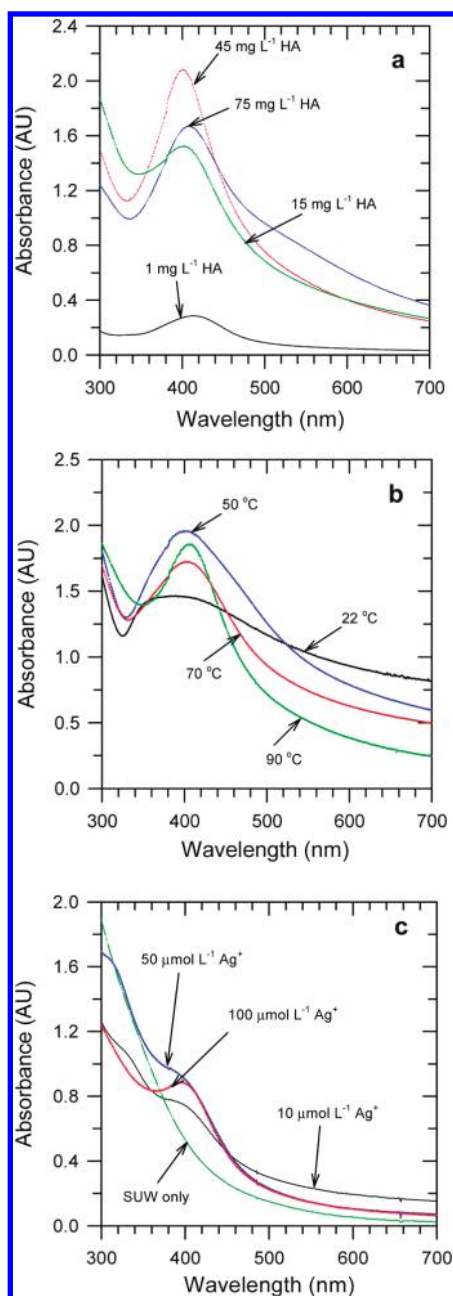
Figure 1. UV-vis absorption spectra of AgNPs in HA. (a) $[Ag^+] = 1 \times 10^{-3}$ mol L^{-1}, reaction times of (90, 120, 330, and 330) min for (75, 45, 15 and 1) mg L^{-1} of [SUW] respectively, $T = 90$ °C (b) different reaction temperatures, $[Ag^+] = 1 \times 10^{-3}$ mol L^{-1}, [SUW] = 100 mg L^{-1}, reaction times of 1 h, 7 h, 4 and 13 days for reactions at (90, 70, 50, and 22) °C, respectively (c) different $[Ag^+]$ of (10, 50, and 100) μmol L^{-1} for reaction time of (11, 4 and 3) h, $T = 90$ °C, [SUW] = 100 mg L^{-1}.

Figure 2. UV-vis absorption spectra of AgNPs; (a) different sedimentary and aquatic HAs. $[Ag^+] = 1 \times 10^{-3}$ mol L^{-1}, reaction times of 8, 9, 12, and 13 days for LD, SR, M2, and SUW respectively, $T = 22$ °C, and [HA] = 100 mg L^{-1}; (b) different sedimentary and aquatic HAs. $[AgNO_3] = 1 \times 10^{-3}$ mol L^{-1}, $T = 90$ °C, reaction times of (1, 0.8, 2, 2, and 3) h for SUW, SUW-1, LD, SR, and M2, respectively, [HA] = 100 mg L^{-1}; (c) different soil HAs, $[AgNO_3] = 1 \times 10^{-3}$ mol L^{-1}, reaction times of 5 h for AL and 24 h for S1, MB, FITJ and WM, $T = 90$ °C, [HA] = 100 mg L^{-1}.

spectroscopy (Figure 1a−c). The peak wavelength location can vary as a function of the diameter and agglomeration state of the AgNPs and the local dielectric environment of the AgNPs (i.e., either the presence of surface molecules or the electrolyte composition of the suspension) (see SI for further details).[31] In this work, the peak characteristics depended on the initial concentration of the HA and temperature of the reaction mixture (Figure 1a−b) impacted by the presence of the HA (HA only spectra are provided for reference in SI Figures SI-1 and SI-2).
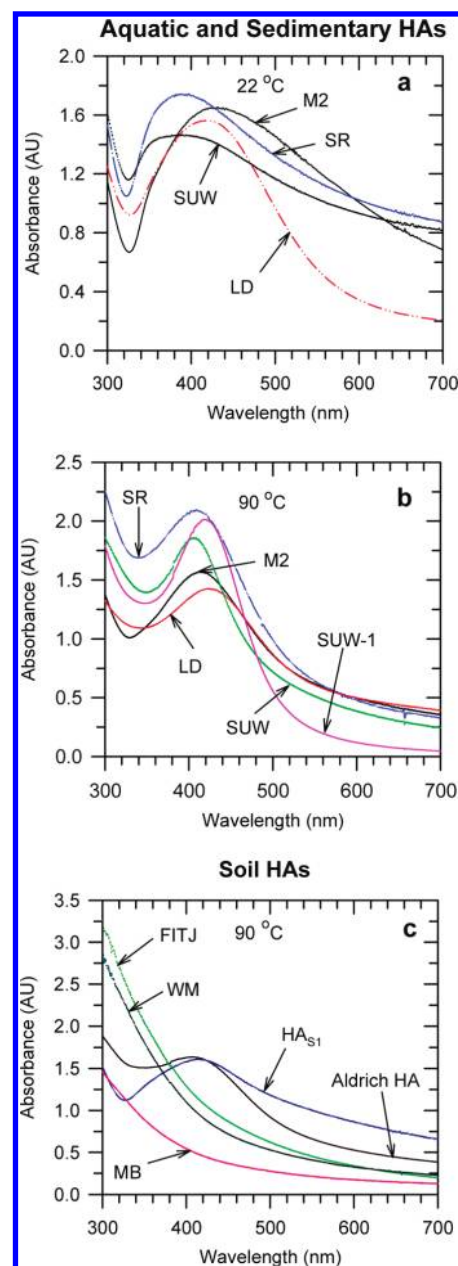
The SPR peak was broader with lower concentrations of HA at a constant Ag^+ concentration and temperature, indicating more polydisperse AgNP size distributions, perhaps due to insufficient quantities of HA required to stabilize small-diameter AgNPs.

An increase in temperature of the reaction mixture with constant $[Ag^+]$ and [HA] promoted growth of AgNPs (resulted in a more intense peak absorbance) and also caused the peak to narrow (Figure 1b). Alternatively, at higher temperatures, an aggregative growth mechanism may be operational

wherein initial molecular Ag-precursors (presumably bound to humic species) can coalesce to form larger clusters. Such clusters can undergo dissolution, recrystallization, and surface reconstruction to yield nanoparticulate species with well-defined SPR peaks. Importantly, the formation of AgNPs also occurred even at $(10-100) \mu$mol L^{-1} of Ag$^+$, although with less pronounced SPR peaks (Figure 1c). Formation of AgNPs by exposure of aqueous Ag$^+$ to HA may proceed by initial complexation followed by reduction of Ag$^+$ to colloidal silver. The reduction potentials of Ag$^+$ and SUW are 0.8 and 0.3 V (vs. saturated calomel electrode), respectively;[32] thus, the formation of silver nuclei from the Ag$^+$ is thermodynamically favored.

Next, the formation of AgNPs was studied using SHAs (M2, SR, and LD) at RT and 90 °C while keeping concentrations of Ag$^+$ and HA constant. The final absorption spectra of the SHA/ AgNP mixtures are presented in Figure 2a–b. Reactions at RT took between 4 and 13 days before a distinct yellow color was observed, while the formation of AgNPs at 90 °C was visually detectable within 90 min. The length of time to achieve an absorbance of approximately 2.0 also varied with the source of the HA. The broad SPR peaks of the AgNPs produced at RT (Figure 2a) indicate broader particle size distributions, in contrast to narrower peaks for reactions carried out at elevated temperature (90 °C). Generally, reactions using HA from sediments are less favorable than the reaction using SUW. Reactions carried out with SUW-1 (solution contained several dissolved ions found in natural aqueous systems such as fresh water) appeared to form AgNPs at approximately similar reaction rates as observed with SUW. However, the SPR peak wavelength of formed AgNPs from SUW-1 was slightly broader and red-shifted to 420 nm in contrast to the 405 nm for SUW formed AgNPs (Figure 2b). This clearly suggests that interference from other ions present in SUW-1 does not substantially modify the HA-induced reduction pathway responsible for formation of Ag nanocrystals.

Soil HAs were also used to form AgNPs at 90 °C. Two soil HAs, of the five tested, reduced Ag$^+$ to AgNPs, but only at the elevated temperature of 90 °C and only after several hours of heating (Figure 2c). No detectable AgNPs were observed after 25 days at RT; hence, experiments at RT were halted. Other natural or sustainable precursors, such as coffee or tea extracts used as both reducing and capping agents, have been reported to synthesize AgNPs at RT.[33] Overall, the present study revealed that the predominant aliphatic-based SHAs and aquatic HA more readily reduced Ag$^+$ to colloidal silver than did aromatic-dominated soil HAs. It is likely due to the presence of the dominant form of reduced organic sulfides (thiols) in SHAs[20] in contrast to the more oxidized form of organic sulfur present in soil HAs.[23] This is also supported by results from a previous study on the redox behavior of different HAs, which found that SUW had a greater reducing capacity than did Peat HA which in turn, was more reducing than Soil HA.[32] It is also possible that the greater conformational rigidity associated with aromatic rings might make functional groups on soil HAs less accessible than those on the more aliphatic aquatic and SHAs.

Characterization of AgNPs. TEM images and SAED data collected for the AgNPs produced in different HA solutions are shown in Figure 3 (M2) and SI Figures SI 3 and 4 (SR). The AgNPs were typically spherical and had a very broad size distribution, ranging from diameters greater than 50 nm to less than 5 nm, or from greater than 10^6 Ag atoms per AgNP to less than 10^4 Ag atoms per AgNP. The larger AgNPs appeared to be relatively more agglomerated, either with other AgNPs or with
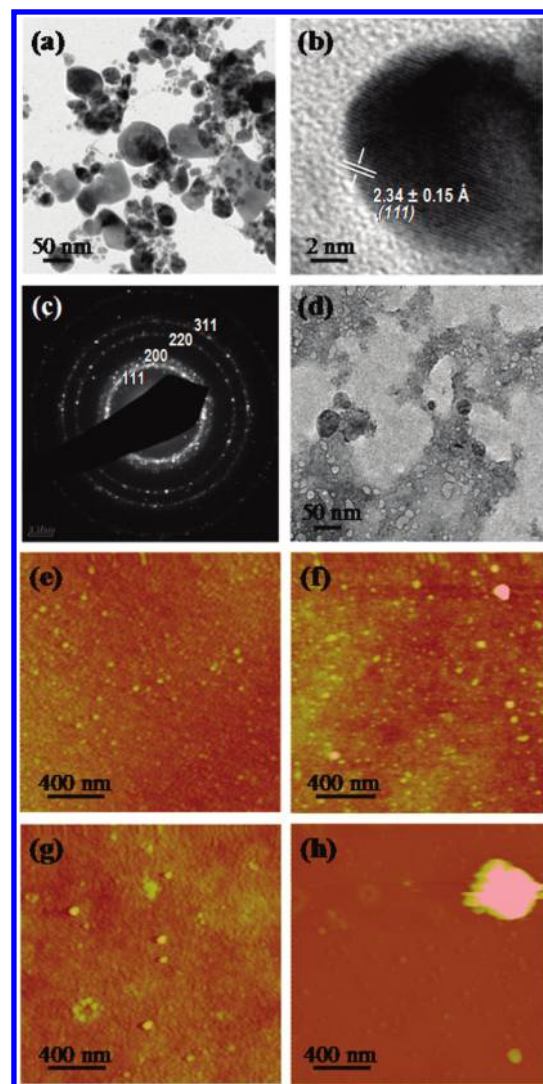

Figure 3. Low-resolution (a) and high-resolution (b) TEM images of the AgNPs produced in the M2 solution with the corresponding SAED pattern (c) of the AgNP. Low-resolution TEM image of the as-prepared M2 solution is shown for comparison (d). The diffraction patterns can be precisely indexed to the face-centered cubic phase of silver (JCPDS no. 040783). AFM image of AgNPs formed by mixing AgNO$_3$ with (e) M2 for 6 days, or (f) SR or (g,h) SUW for 13 days at RT. Z-scale is 10 nm in (e–g) and 250 nm in (h).

the HA natural colloids, supported by the AFM results, which minimize drying induced agglomeration, discussed later. Lattice-resolved images (Figure 3b, and SI Figures 3b and 4b) and SAED data (Figure 3c, and SI Figures 3c and 4c) confirm the presence of crystalline AgNPs in the samples that are not present in the control. Figure 3b clearly illustrates the [111] growth direction of the AgNPs. The indexed concentric diffraction rings in the SAED pattern were observed for the AgNP samples synthesized in different HA solutions, indicating the presence of crystallites including those that are perhaps embedded within the natural colloids and escape detection in atomic resolution HRTEM imaging (Figure 3c). The SAED patterns and lattice planes observed in HRTEM imaging can be indexed to face-centered cubic silver metal as per Joint Committee on Powder Diffraction Standards (JCPDS) Card no. 040783. The caveat in extracting size distributions from low-resolution TEM images is that there is

Table 1. Physical Characteristics of AgNPs Formed under Different Conditions, Observed by DLS[a]

sample	mean Z_{avg} (nm)	stdev Z_{avg} (nm)	mean PI	stdev PI	count rate (counts per second)
SR, RT	74.5	1.4	0.287	0.022	262 996
M2, RT	90.5	3.4	0.281	0.009	447 871
SUW, RT	82.8	3.3	0.405	0.038	481 552
SUW 90 °C, 90 min	130.3	4.2	0.337	0.043	58 106
M2 90 °C, 3 h	158.5	4.3	0.300	0.016	83 598
SR alone	251	14	0.537	0.135	1377
SUW alone	856	53	0.472	0.097	539
M2 alone	748	102	0.720	0.090	426

[a] The mean of five measurements with one standard deviation is reported.

clearly a large abundance of amorphous natural colloids with equivalent electron density (Figure 3d).

AFM images were collected for the AgNPs produced by incubating 1 mmol L^{-1} silver nitrate at RT in HA solutions of M2 for 6 days (Figure 3e), SR for 13 days (Figure 3f), and SUW for 13 days (Figure 3g—h). Singly dispersed spherical particles, mostly less than 10 nm in diameter, are visible in all three samples. Infrequently, images contained larger diameter particles that were less spherical, such as those observed in Figure 3f, or large agglomerates of many particles, such as those observed in Figure 3h.

Table 1 provides a summary of the DLS data collected (SI Figures SI-5—SI-12 for intensity-based size-distributions). The mean hydrodynamic diameter of the AgNPs produced with M2, SR, or SUW at RT ranged from 74.5 to 90.5 nm, while those produced at 90 °C from the SUW were significantly larger, ranging from 130.3 to 158.5 nm. The polydispersity index (PI) of the AgNPs was greater than 0.3 in most cases, suggesting a polydisperse size distribution. When considering that DLS intensity follows Raleigh scattering and is thus proportional to the radius of the particle raised to the sixth power, a small number of large AgNPs can contribute significantly to the intensity-based DLS size, thus the larger hydrodynamic diameters and PIs do agree with the AFM and TEM imaging results. Based in Table 1, it is likely that at higher temperatures, a very small number of larger AgNPs or agglomerates of AgNPs are present in the suspensions, and thus readily observed by DLS. These are likely a result of the accelerated reduction which causes rapid particle growth at high temperatures. As the microscopy results are number-based size distributions, these combined results highlight the advantages of combining multiple size measurement methods (such as DLS and microscopies) to provide a more detailed understanding of the true nature of the size distributions of NP suspensions.

The DLS size of the HAs alone, at the concentrations used for the reactions, was several hundreds of nanometers in diameter and very polydisperse (PI greater than 0.4). Additionally, detector count rates were orders of magnitude less than suspensions containing AgNPs, suggesting either the HA particles have a poor scattering efficiency or there was a smaller number or volume fraction of HA particles present in the solution. This suggests that any interferences from the HA particles on the observed DLS autocorrelation function, and thus the calculated hydrodynamic size of the AgNPs, should be minimal.

Environmental Implications. The results of this study demonstrate that AgNPs could potentially be formed from aqueous Ag$^+$ exposed to HAs at environmentally relevant conditions (1—5 mg L^{-1} HA, pH 7.4—8.1, RT). Several reports have attributed the increase in levels of AgNPs in aqueous

environments to increased production and mobilization of silver nanomaterials.[8,15,34] Also, the major portion of dissolved silver was found to be associated with macromolecular organic matter,[14] suggesting its involvement in the formation of Ag colloids. Some AgNPs in aqueous environments could potentially arise from the interaction between HA and dissolved Ag$^+$, be they ions originating from bulk sources or from oxidation of AgNPs.[11,35] If this is the case, then it is likely that AgNPs that leach into aqueous environments could remain in this form, in part due to a colloidal-stabilizing interaction with HAs, and in part due to reduction of Ag$^+$ that may have resulted from oxidation of AgNPs themselves. An important implication of this finding to the fate and transport of engineered nanomaterials is the demonstration that ions leached from any silver metal source can form NPs under the appropriate environmental conditions. If this hypothesis is correct, in areas where production and use of AgNPs is modest, there could still be significant levels of AgNPs in the aqueous environment as a result of HA reduction of Ag$^+$ from sources such as leachates from silver mine tailings[35] and photographic waste-water. Furthermore, the results obtained at elevated temperatures suggest that if a Ag$^+$ source was present in naturally occurring environments with elevated temperatures, such as thermal vents or hot-springs, which are known to have elevated dissolved silver levels,[25] it may be possible for AgNPs to form rapidly.

The presence of HA could create an oxidation and reduction cycle of dissolution and reappearance of AgNPs in certain aquatic compartments as well as new mechanisms of persistence. Particles could undergo chemical oxidation and reconstitution, or they could aggregate and settle out, and then be reoxidized, followed by sequential leaching from soils as Ag$^+$, which could be reconstituted into AgNPs by HA. This phenomenon might explain the presence of silver as nanoparticles in an old silver mining region of Zacatlan, Puebla, Mexico[35] and earlier reported presence of colloidal silver in fluvial and estuarine waters of Texas[14] prior to widespread use of AgNPs in consumer products. However, in regions of low concentration of silver in the environment, the reduction of Ag$^+$ by HA is likely to be slow, although the mechanistic pathways identified here will still generally be valid. Similarly, oxidation of AgNPs by other oxidants will vary considerably depending on the redox activity and concentration of the oxidizing agents. Under such conditions, lower levels of AgNPs would exist because most of the silver would likely be present in the form of dissolved Ag$^+$.

Experiments were conducted in capped glass test tubes to further evaluate the stability of the HA-formed AgNPs on a longer time scale. Formed AgNPs were always stored in capped vials however, since the vials were opened periodically to remove aliquots for UV-vis analysis, it would replenish the headspace
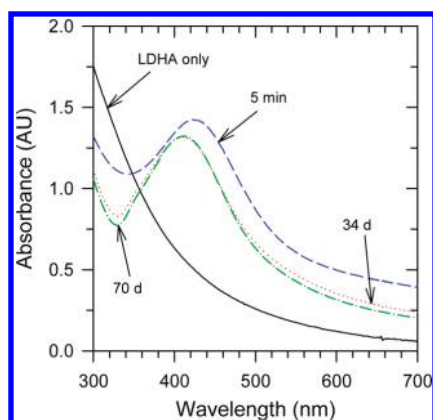
Figure 4. Stability studies of UV-vis absorption spectra of AgNPs following reduction of silver nitrate solution with LD as described in Figure 2a. Absorption spectra of the AgNPs were acquired 5 min, 34 min, and 70 days after formation of the AgNPs.

oxygen each time, reducing the likelihood that results would have been different if samples were open, as the kinetics of partial AgNP dissolution is typically on the time scale of several weeks to months. As shown in Figure 4, the AgNPs formed by reaction with HA from LD indicated only a 7% decrease in the SPR peak intensity after a period of 70 days. The SPR peak of LD AgNPs also blue-shifted from 423 to 410 nm during this time, and may be related to oxidation of AgNPs. A decrease of 6% in the SPR peak intensity was observed for AgNPs formed from reaction with SR after 70 days with no observable shift in the SPR peak wavelength and intensity. AgNPs formed from interaction with SUW constituted the only case in which a significant decrease (25%) in SPR peak intensity was observed after 70 days with no shift in SPR peak wavelength. In contrast, the SPR peak for AgNPs formed from interaction with M2 consistently increased in intensity during the entire experiment duration (70 days). However, our results suggest that AgNPs formed from the interaction with sedimentary HAs are quite stable over a significant time period, which could allow them to be transported for long distances from their location of origin. Indeed, to the best of our knowledge, sequential leaching and reconstitution of engineered nanomaterials has thus far not been considered in most models for environmental transport, and there may be a more complex pattern of AgNP transport in the environment than previously thought.

ASSOCIATED CONTENT

Ⓢ **Supporting Information.** Figures SI-1–SI-13, Table S1, and additional text. This material is available free of charge via the Internet at http://pubs.acs.org.

AUTHOR INFORMATION

Corresponding Author
*Phone: 321-674-7310; fax: 321-674-8951; e-mail: vsharma@fit.edu.

ACKNOWLEDGMENT

REFERENCES

(1) Sharma, V. K.; Yngard, R. A.; Lin, Y. Silver nanoparticles: Green synthesis and their antimicrobial activities. *Adv. Colloid Interface Sci.* **2009**, *145*, 83–96.

(2) Sotiriou, G. A.; Pratsinis, S. E. Antibacterial activity of nanosilver ions and particles. *Environ. Sci. Technol.* **2010**, *44*, 5649–5654.

(3) Wigginton, N. S.; de Titta, A.; Piccapietra, F.; Dobias, J.; Nesatyy, V. J.; Suter, M. J. F.; Bernier-Latmani, R. Binding of silver nanoparticles to bacterial proteins depends on surface modifications and inhibits enzymatic activity. *Environ. Sci. Technol.* **2010**, *44*, 2163–2168.

(4) FIFRA Scientific Advisory Panel Meeting Evaluation of the hazard and exposure associated with nanoparticles and other nanometal pesticides and products. www.epa.gov/scipoly/sap/meetings/2009/november/110309ameetingminutes.pdf.

(5) Lee, K. J.; Nallathamby, P. D.; Browning, L. M.; Osgood, C. J.; Xu, X. H. N. In vivo imaging of transport and biocompatibilty of single silver nanoparticles in early development of zebrafish embryos. *ACS Nano* **2007**, *1*, 133–143.

(6) Harper, S.; Usenko, C.; Hutchison, J. E.; Maddux, B. L. S.; Tanguay, R. L. In vivo biodistribution and toxicity depends on nano-material composition, size, surface functionalisation and route of exposure. *J. Exp. Nanosci.* **2008**, *3*, 195–206.

(7) Figueroa, J. A. L.; Wrobel, K.; Afton, S.; Caruso, J. A.; Gutierrez Corona, J. F.; Wrobel, K. Effect of some heavy metals and soil humic substances on the phytochelatin production in wild plants from silver mine areas of Guanajuato, Mexico. *Chemosphere* **2008**, *70*, 2084–2091.

(8) Eckelman, M. J.; Graedel, T. E. Silver emissions and their environmental impacts: A multilevel assessment. *Environ. Sci. Technol.* **2007**, *41*, 6283–6289.

(9) Elzey, S.; Grassian, V. H. Agglomeration, isolation and dissolution of commercially manufactured silver nanoparticles in aqueous environments. *J. Nanopart. Res.* **2010**, *12*, 1945–1958.

(10) Pal, S.; Tak, Y. K.; Song, J. M. Does the antibacterial activity of silver nanoparticles depend on the shape of the nanoparticle? A study of the gram-negative bacterium *Escherichia coli. Appl. Environ. Microbiol.* **2007**, *73*, 1712–1720.

(11) Liu, J.; Hurt, R. H. Ion release kinetics and particle persistence in aqueous nano-silver colloids. *Environ. Sci. Technol.* **2010**, *44*, 2169–2175.

(12) El Badawy, A. M.; Luxton, T. P.; Silva, R. G.; Scheckel, K. G.; Suidan, M. T.; Tolaymat, T. M. Impact of environmental conditions (pH, ionic strength, and electrolyte type) on the surface charge and aggregation of silver nanoparticles suspensions. *Environ. Sci. Technol.* **2010**, *44*, 1260–1266.

(13) Fabrega, J.; Fawcett, S. R.; Renshaw, J. C.; Lead, J. R. Silver nanoparticle impact on bacterial growth: effect of pH, concentration, and organic matter. *Environ. Sci. Technol.* **2009**, *43*, 7285–7290.

(14) Wen, L.; Santschi, P. H.; Gill, G. A.; Paternostro, C. L.; Lehman, R. D. Colloidal and particulate silver in river and estuarine waters of Texas. *Environ. Sci. Technol.* **1997**, *31*, 723–731.

(15) Benn, T. M.; Westerhoff, P. Nanoparticle silver released into water from commercially available sock fabrics. *Environ. Sci. Technol.* **2008**, *42*, 4133–4139.

(16) Blaser, S. A.; Scheringer, M.; MacLeod, M.; Hungerbuehler, K. Estimation of cumulative aquatic exposure and risk due to silver: Contribution of nano-functionalized plastics and textiles. *Sci. Total Environ.* **2008**, *390*, 396–409.

(17) Kramer, J. R.; Benoit, G. Environmental chemistry of silver. In *Silver in the Environment: Transport, Fate, and Effects*. Andren, A. W., Bober, T. W., Eds. SETAC Press: North Carolina, 1993; pp 1–47.

(18) Sal'nikov, D. S.; Pogorelova, A. S.; Makarov, S. V.; Vashurina, I. Y. Silver ion reduction with peat fulvic acids. *Russ. J. of Appl. Chem.* **2009**, *82*, 545–548.

(19) Stevenson, F. J. *Humic Chemistry: Genesis, Composition, Reactions*. Wiley: New York, 1994.

(20) Urban, N. R.; Ernst, K.; Bernasconi, S. Addition of sulfur to organic matter during early diagenesis of lake sediments. *Geochim. Cosmochim. Acta* **1999**, *63*, 837–853.

(21) Ishiwatari, R. Estimation of the aromaticity of a lake sediment humic acid by air oxidation and evaluation of it. *Soil Sci.* **1969**, *107*, 53–57.

(22) Nissenbaum, A.; Swaine, D. J. Organic matter-metal interactions in Recent sediments: the role of humic substances. *Geochim. Cosmochim. Acta* **1976**, *40*, 809–816.

(23) Lehmann, J.; Solomon, D.; Zhao, F.; McGrath, S. P. Atmospheric SO_2 Emissions Since the Late 1800s Change Organic Sulfur Forms in Humic Substance Extracts of Soils. *Environ. Sci. Technol.* **2008**, *42*, 3550–3555.

(24) Hatcher, P. G.; Maciel, G. E.; Dennis, L. W. Aliphatic structure of humic acids; a clue to their origin. *Org. Geochem.* **1981**, *3*, 43–48.

(25) *Ambient Water Quality Criteria for Silver*, Highlights of 440/5-80-071; United States Environmental Protection Agency: Washington, DC, 1980; water.epa.gov/water404.cfm.

(26) Sohn, M. L.; Hughes, M. C. Metal ion complex formation constants of some sedimentary humic acids with zinc(II), copper(II), and cadmium(II). *Geochim. Cosmochim. Acta* **1981**, *45*, 2393–2399.

(27) Hayes, M. H. B. *Extraction of Humic Substances from Soil: Humic Substances in Soil, Sediment and Water-Geochemistry, Isolation and Characterization*; Wiley: New York, 1885.

(28) *Methods for Measuring the Acute Toxicity of Effluents and Receiving Waters to Freshwater and Marine Organisms*, Highlights of 600/4-90/027F; United States Environmental Protection Agency: Washington, DC, 1993; www.epa.gov/waterscience/methods/wet/disk2/atx.pdf.

(29) Hackley, V. A. Clogston, J. D. *NIST - NCL Joint Assay Protocol PCC-1: Measuring the Size of Nanoparticles in Aqueous Media Using Batch-Mode Dynamic Light Scattering*; National Institute of Standards and Technology: Gaithersburg, MD, 2007; ncl.cancer.gov/working_assay-cascade.asp.

(30) Grobleny, J.; Delrio, F. W.; Pradeep, N.; Kim, D.; Hackley, V. A.; Cook, R. F. *NIST - NCL Joint Assay Protocol, PCC-6: Size Measurement of Nanoparticles Using Atomic Force Microscopy*; National Institute of Standards and Technology: Gaithersburg, MD, 2009; ncl.cancer.gov/working_assay-cascade.asp.

(31) Duan, J.; Park, K.; MacCuspie, R. I.; Vaia, R. A.; Pachter, R. Optical properties of rodlike metallic nanostructures: Insight from theory and experiment. *J. Phys. Chem. C* **2009**, *113*, 15524–15532.

(32) Struyk, Z.; Sposito, G. Redox properties of standard humic acids. *Geoderma* **2001**, *102*, 329–346.

(33) Nadagouda, M. N.; Varma, R. S. Green synthesis of silver and palladium nanoparticles at room temperature using coffee and tea extract. *Green Chem.* **2008**, *10*, 859–862.

(34) Alvarez, P. J. Nanotechnology in the environment - The good, the bad, and the ugly. *J. Environ. Eng* **2006**, *132*, 1233.

(35) Liu, J.; Sonshine, D. A.; Shervani, S.; Hurt, R. H. Controlled release of biologically active silver from nanosilver surfaces. *ACS Nano* **2010**, *4*, 6903–6913.

(36) Gomez-Caballero, J. A.; Villasenor-Cabral, M. G.; Santiago-Jacinto, P.; Ponce-Abad, F. Hypogene Ba-rich todorokite and associated nanometric native silver in The San Miguel Tenango mining area, zacatlan, puebla, Mexico. *Can. Mineral* **2010**, *48*, 1237–1253.